25090.1-EG-SBI

ANALYTICAL METHODS REPORT 8801

(2)

DEVELOPMENT OF A PANEL METHOD FOR MODELING CONFIGURATIONS WITH UNSTEADY COMPONENT MOTIONS

PHASE I FINAL REPORT

PREPARED UNDER SBIR CONTRACT DAAL03-87-C-0011

Prepared By:

David R. Clark & Brian Maskew

Analytical Methods Inc.
2133 152nd Avenue N.E.
Redmond, Washington 98052
(206) 643-9090

Prepared For:

U.S. Army Research Office
P.O. BOX 12211
Research Triangle Park, N.C. 27709-2211

April 1988

UNCLASSIFIED
SECURITY CLASSIFICATION OF THIS PAGE

REPORT DOCUMENTATION PAGE

1a. REPORT SECURITY CLASSIFICATION Unclassified	1b. RESTRICTIVE MARKINGS
2a. SECURITY CLASSIFICATION AUTHORITY	3. DISTRIBUTION/AVAILABILITY OF REPORT Approved for public release; distribution unlimited.
2b. DECLASSIFICATION/DOWNGRADING SCHEDULE	
4. PERFORMING ORGANIZATION REPORT NUMBER(S)	5. MONITORING ORGANIZATION REPORT NUMBER(S)
6a. NAME OF PERFORMING ORGANIZATION Analytical Methods Inc 6b. OFFICE SYMBOL (If applicable) -------	7a. NAME OF MONITORING ORGANIZATION U. S. Army Research Office
6c. ADDRESS (City, State, and ZIP Code) 2133 152nd Ave N.E. Redmond, WA 98052	7b. ADDRESS (City, State, and ZIP Code) P. O. Box 12211 Research Triangle Park, NC 27709-2211
8a. NAME OF FUNDING/SPONSORING ORGANIZATION U. S. Army Research Office 8b. OFFICE SYMBOL (If applicable)	9. PROCUREMENT INSTRUMENT IDENTIFICATION NUMBER DAAL03-87-C-0011
ADDRESS (City, State, and ZIP Code) P. O. Box 12211 Research Triangle Park, NC 27709-2211	10. SOURCE OF FUNDING NUMBERS PROGRAM ELEMENT NO. / PROJECT NO. / TASK NO. / WORK UNIT ACCESSION NO.
11. TITLE (Include Security Classification) Development of a panel method for modeling configurations with unsteady component motions -Unclassified-	
12. PERSONAL AUTHOR(S) David R. Clark & Brian Maskew	
13a. TYPE OF REPORT Final	13b. TIME COVERED FROM 7/1/87 TO 1/31/88
14. DATE OF REPORT (Year, Month, Day) April 15th, 1988	15. PAGE COUNT 31
16. SUPPLEMENTARY NOTATION The view, opinions and/or findings contained in this report are those of the author(s) and should not be construed as an official Department of the Army position, policy, or decision, unless so designated by other documentation.	

17. COSATI CODES			18. SUBJECT TERMS (Continue on reverse if necessary and identify by block number)
FIELD	GROUP	SUB-GROUP	

19. ABSTRACT (Continue on reverse if necessary and identify by block number)

This report reviews the background to the calculation of unsteady rotor and fuselage loads and presents results from an analysis of a typical helicopter configuration made using a panel method operated in a time-stepping mode. The method models the fuselage and blades using surface singularities and the shed and trailing wakes with doublet lattice sheets. Unsteady local pressures and component forces are presented and the ability of the analysis to determine dynamic phenomena such as fuselage/blade-passage events and blade/vortex interactions is demonstrated.

20. DISTRIBUTION/AVAILABILITY OF ABSTRACT ☒ UNCLASSIFIED/UNLIMITED ☒ SAME AS RPT. ☐ DTIC USERS	21. ABSTRACT SECURITY CLASSIFICATION Unclassified
22a. NAME OF RESPONSIBLE INDIVIDUAL	22b. TELEPHONE (Include Area Code) / 22c. OFFICE SYMBOL

DD FORM 1473, 84 MAR 83 APR edition may be used until exhausted. All other editions are obsolete.

SECURITY CLASSIFICATION OF THIS PAGE
UNCLASSIFIED

TABLE OF CONTENTS

LIST OF FIGURES

1.0 INTRODUCTION

Even before the advent of the helicopter in its modern (post World War II) form, the mathematical treatment of unsteady blade loads was already quite advanced. The success of this early work by Glauert (1), (2) and others, and later by Wheatley (3) can be measured by the fact that the methods they laid down are still used as a standard for comparison when new approaches are being considered (4). Limited by their inability to properly predict the extent of regions of stall and by the inevitable assumption regarding inflow, they nonetheless, in the pre-computer era, provided reliable predictions of blade radial and azimuthal load variation.

As the computer reached practical maturity in the 1960s a new family of approaches to blade loads became available. These approaches, typified by the work of References (5) through (9), employed a lifting line model for the blade and were able to provide more realistic representation of the inflow velocities through the use of a vortex filament model of the wake. These models were initially prescribed as skewed helices whose trajectory was based on simple momentum arguments. With this approach the user was better able to predict the higher harmonics of loading coming from blade/vortex encounters around the azimuth. These approaches inevitably suffered from the assumptions made in the initial positioning of the wake.

Development of methods for simultaneously calculating wake position, using a time-stepping approach, and blade performance considerably improved the accuracy of airloads prediction. The work of Landgrebe and others (10) - (14) is typical of the methods developed. Despite the improved ability to predict the rotor inflow distribution offered by the new methods they still suffered from the basic limitations of blade element theory. In particular, the use of steady, two-dimensional airfoil data as the basis for the loads and performance calculation was a very obvious limitation when the unsteady, distinctly three-dimensional flow field of the helicopter rotor is being considered. Treatments of the unsteady and yawed effects were developed, Refs. 15 and 16 are typical, but the lifting line, vortex filament models of the rotor flow field still have not been able to reliably predict the performance of rotors in forward flight (4), particularly for conditions close to the limits of the rotor flight envelope.

While the radial and azimuthal variations of blade loading produced by the lifting line/blade element models were generally adequate for performance predictions and were acceptable for dynamic loads work when detailed blade section pitching moment data were available, they would not provide the chordwise blade loading variation that is necessary for detailed blade dynamics and essential for accurate noise prediction. This is a fundamental limitation of the blade element-lifting line approach.

Methods to provide this missing component, the chordwise load variation, come from classical potential flow theory. Developed first in a practical form (but for non-lifting bodies) by Hess and Smith (17), the methods were extended using thin surface or full surface singularity models to solve the problem of determining the behavior of lifting shapes in steady rectilinear flight. The work of Refs. 18 and 19 is typical. Unfortunately, the environment of the helicopter rotor blade is neither steady nor is it rectilinear and this problem was addressed by a number of authors. References 20 through 23 are typical of this work. The dramatic effect that changing from a lifting line to a lifting surface model can have on predicted loads is best illustrated in the work of Johnson (24) where the excursions in dynamic blade loading are seen to be dramatically different with the lifting surface approach and the chordwise relief it provides.

Other authors have explored the use of lifting surface models. Notable is the work of Dat and his colleagues at ONERA (25), (26). Using a doublet lattice approach they were able to substantially improve the correlation between predicted and measure dynamic blade loads over earlier methods.

Lifting surface approaches, even when they effectively model the distribution of blade loads, neglect a factor which becomes more and more important as tip speed increases; that is, blade thickness. Without including the effect of thickness in the calculation, true local velocities, and hence, incipient transonic flow events cannot be determined. Further, without a "real" model of the surface, streamline and viscous flow behavior cannot be determined and it is not possible to identify regions of laminar or turbulent flow or to predict possible boundary layer separation. For this task a full surface singularity model is required.

In an attempt to better define the high subsonic and transonic flow regions on the rotor, several workers have taken advantage of the advances in computer capability to explore full potential and finite difference approaches. These two approaches are typified by the work of Tauber in Refs. 27 and 28 which extends the fixed wing approach of Jameson (29) to rotor cases, and the work of Caradonna and his associates in Refs. 30 through 32. While early results with those and other similar approaches, Ref. 33 for example, have been encouraging, they are at this stage far from being practical engineering tools. Apart from the purely mechanical problems of grid generation in a flow field whose characteristics are not very well defined and where there is a very large spread of significant length scales, the methods rely on the results of existing wake modeling techniques to specify the boundary conditions on their solution domains. As a result of this they fall prey to and must be sensitive to all of the probblems that affect the earlier, more elementary approaches. These comments apply equally to today's methods and the hybrid Euler and Navier-Stokes approaches now being considered. References 34 and 35 typify this work.

Another factor, beyond blade/vortex interactions and response of a section to inflow variations, contributes to blade dynamic loading. That is, the influence of the fuselage on the blade as it tracks around the azimuth. Highlighted in the work of Sheriden (36), "interactional aerodynamics" drew attention to the strong influence the other components of the vehicle can have on blade loads and how the dynamics of blade passage dominate the fuselage airloading. The significance of these effects became very evident in the generation of helicopters developed in the 1970s. These machines, designed to meet an air transportability requirement, all were rolled out with low mast heights and, as a consequence, close blade/fuselage passage. All were subsequently redesigned with increased rotor height to reduce the unfavorable effects of the blade/fuselage interference. Reference 37 documents an analysis of this problem. Using an early panel method to model the fuselage (38), the authors presented contours of fuselage-induced velocities in the plane of the rotor and, working with a separate lifting line/ vortex filament wake model were able to evaluate fuselage on rotor effects. Later treatments (39), (40), looked at the problem from other aspects, even (as in Refs. 41 and 42) to the extent of allowing for coupling of the fuselage loads, determined by a full surface singularity panel method and rotor loads, from a blade element model to give not only body-on-roter but also rotor-on-body effects. None of these methods, however, goes beyond a lifting line model of the blade or a vortex or doublet lattice model of the wake.

The work of Cantaloube (43) is significant in that it presents results for a simultaneous solution of fuselage and blade loads for a helicopter in forward flight. Using a truncated panel model for the fuselage and a lifting surface blade model, he was able to calculate the blade wake development in the presence of the body. No unsteady surface loads were presented in Ref. 43 and the use of a lifting surface blade model neglects thickness effects and precludes the identification of transonic flow regions. The use of an open fuselage model with no apparent base wake raises questions regarding the ability of the body to carry lift and to respond to dynamic load variations induced by blade passage.

The present work was carried out to develop a surface singularity model of both fuselage and blades, including wake dynamics, which would provide the basis for a calculation of rotor and fuselage steady and transient loads including (eventually) transonic and viscous flow effects. A primary goal was the development of an engineering analysis which would not require laborious data input preparation or grid generation effort and which would be, as far as possible, easy to use and economical from the point of view of computation cost.

This report documents the development of the analysis from the steady panel code which preceded it (44), and demonstrate the ability of the code to calculate unsteady fuselage and blade loads for a helicopter flying along a generalized flight path. The wake from each blade, including a fully modeled inboard sheet, is allowed to develop freely in the presence of the body and under the influence of the other blades and their wakes. Even with the relatively crude model used in these initial stages the analysis has been able to capture the details of the passage of individual blades across the fuselage; the rolling blade tip vortex/front fuselage encounter and the more elusive blade/vortex interactions both on the advancing and retreating sides.

2.0 DEVELOPMENT OF THE METHOD

The primary goal of the study was the demonstration of the viability of a panel method operating in a time-stepping mode as a tool for investigating transient aerodynamic events. A panel method was chosen for this work since it was felt that it offered the best chance of providing a practical engineering tool in the (relatively) short term. Other available methods, such as the Euler approach, were thought to be impractical because of the effort involved in developing the required computational mesh at each step in a flow field where such a wide range of length scales was present. These scales could range, in fact, from the aircraft length, in full vehicle maneuvers, to fractions of a blade chord in a blade vortex interaction. Both of these, of course, could be occurring simultaneously in the same application. The grid generation problem is intensified by the time varying geometry in the case of a helicopter rotor or propeller problem. The panel method with its direct surface modeling feature and an ability to resolve details as small as panel density and computing machine capacity permits seems ideally suited to the task.

The method selected as the basis for the present study was developed from the low-order, second generation analysis, program VSAERO (for Vortex Separation AEROdynamics). VSAERO (44) uses a combination of constant source and doublet singularities applied over flat quadrilateral panels to model general surfaces. The doublet term is the unknown in the solution, with the source term being determined from the local component of the free stream velocity normal to the surface. The doublet term, a scalar, is determined by applying the Dirichlet boundary condition and is subsequently differentiated over the surface to produce the local velocities. Wakes are modeled using piecewise constant doublet panel sheets. This analysis had been used with some success to predict body/rotor coupling, where the rotor wake was modeled using a time-averaged vortex sheath (41). This provided unsteady fuselage-on-rotor effects, but because of the time-averaging assumption, rotor-on-body effects were limited to the steady terms.

2.1 Program Modification

Program VSAERO had been extended into the time domain (45) for the study of rotor blade-tip shapes and later for aircraft maneuvers (46). This work proceeded in parallel with a detailed development of the principles involved in dynamic wake modeling using a two-dimensional pilot code (47). Results from this work, published in Refs. 48 and 49, showed that a panel method could be used with confidence to predict dynamic flow effects, even including the development and growth of large regions of separated flow. The work with the pilot code and full vehicle studies coalesced in a new program, designated USAERO (for UnSteady AERODynamics). This program was the jumping off point for the present study.

The basic motion features of the original program were retained. In this, Figure 1, the primary body, here the helicopter fuselage, carries a body-centered coordinate system as it is allowed to move through the controlling inertial frame. Attached to the body may be other components which can have, in addition to the overall body motion, independent motions of their own. These motions may be translational or, as is more generally the case in the configurations of interest here, rotational.

The primary rotation is about the blade shaft axis and provision has been made in the code for each component to have up to 10 superimposed motion schedules which will initially be forced (such as blade cyclic, simple or compound pitch changes) or at some later stage free (such as blade flap and lag motions in response to fluctuating loads). Figure 2 illustrates how these motions are superimposed. Required additional input for the program beyond the body shape is simply a schedule of motions, arranged hierarchically together with an indication of the components involved. The ability to position specified shapes anywhere in the field and to automatically generate the surface paneling is one of the strongest features of the original VSAERO program and this has been retained.

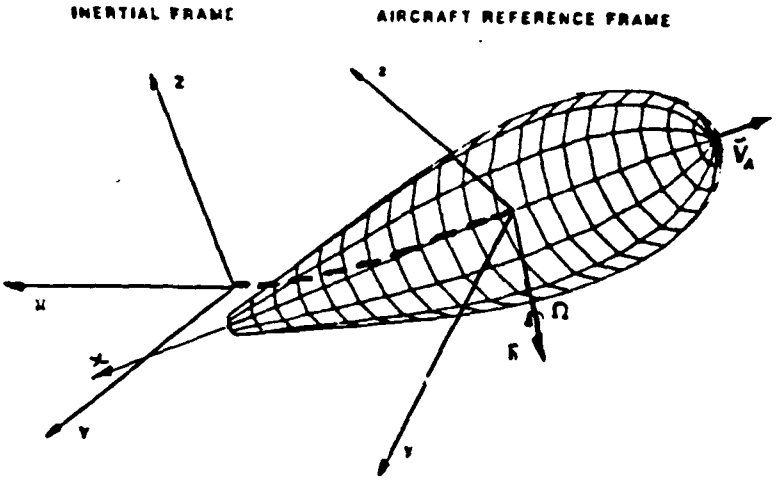

Fig. 1. Aircraft Movement Relative to the Inertial Frame.

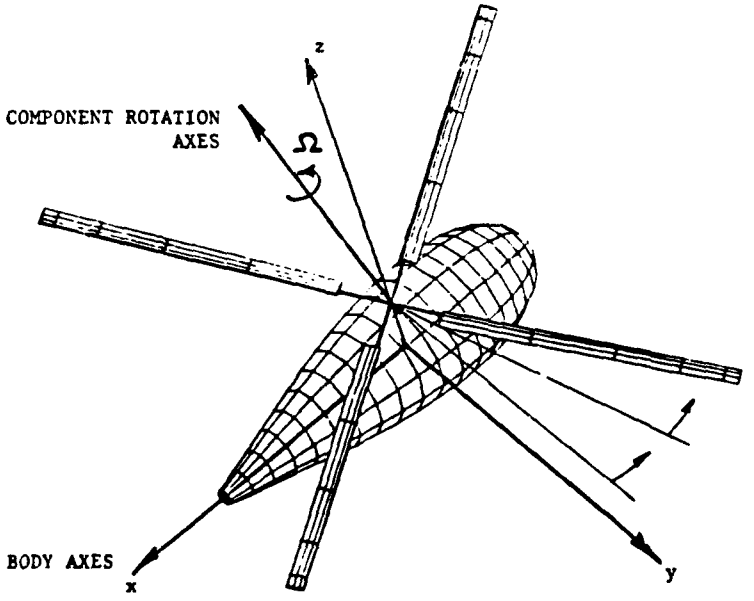

Fig. 2. Schematic of Component Rotation Axes.

One of the most time consuming operations in the earlier program is the calculation of the influence of each panel on every other panel. This is a necessary prelude to the application of the boundary conditions and the inversion and solution of the matrix equation to provide the strengths of the surface singularities. In earlier (even unsteady) work this needed to be performed only once for the body since the geometry remained constant. Only the effects of the wake on the body and on itself had to be determined at each time step (see sketch below). Body-on-body effects remain constant with time.

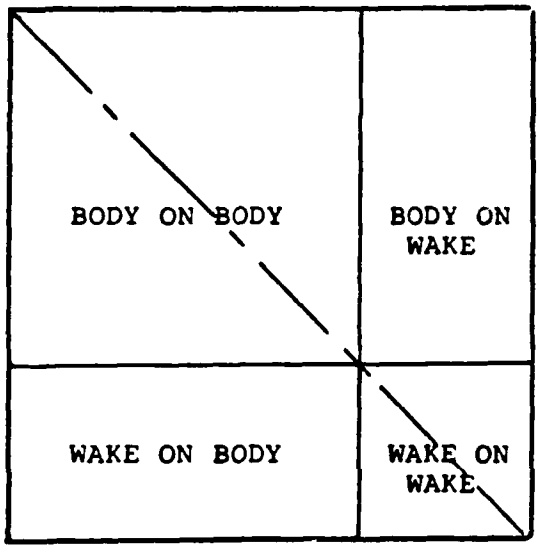

Now, However, where relative motion of individual components is allowed, the matrix of influence coefficients changes from step to step as the relative position of each component changes. Even here, however, the effect of each component on itself remains constant with time. In the sketch below, where A, B and C represent the components of the body, the diagonal terms, A on A, B on B, etc. remain constant from step to step and only the off-diagonal terms need to be re-evaluated.

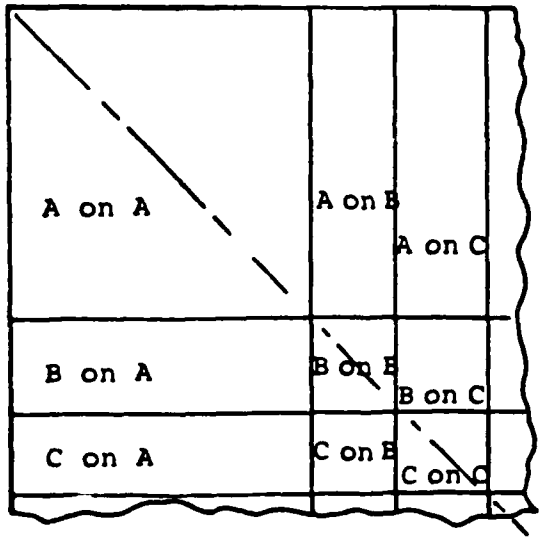

This scheme was incorporated in the program and a considerable reduction in computation time was noted. For the small test cases run during this phase, a typical savings of roughly 40% was found in the influence coefficient calculation when only the off-diagonal influences were recalculated at each step. In this case the moving panels made up about 30% of the total. Savings would be proportionately larger as the moving panels approach 50% of the total.

2.2 Changes to Improve Computation Efficiency

Calculation of even steady state aerodynamics of a configuration using a detailed panel model involves considerable computer resources and if iterative solutions with wake relaxation are considered, long execution times, even on today's fast machines, are a fact of life. When the time domain is entered and these calculations must be repeated many times over, perhaps hundreds of times if fine detail is to be resolved, then computation times could easily become prohibitive. Although the models in this initial study were deliberately kept simple and small and time steps kept to a level sufficient to demonstrate the model, computation over 85 time steps would consume 58,000 CP seconds on a MicroVAX II (about 16 hours) or approximately half a CPU hour on a CRAY. These times were not unexpected, based on a wide experience with panel methods, and ways to reduce computation time received considerable study.

Several promising candidate modifications were determined and these are listed below.

1) Influence coefficient calculation streamlined to minimize calculation of square root, alog and atan terms.

2) Discrimination between far and near field calculation zones done on the basis of atan argument rather than absolute distance.

3) Wake representation changed from quadrilateral to triangle pair form.

4) Wake close passage testing carried out more efficiently.

5) Wake computation all carried out "in core" resulting in large I/O savings.

6) Revise matrix solution scheme saving inverse of those portions not changing from step to step and re-multiplying partitioned matrix after inserting new influence coefficient blocks, Ref. 43.

Overall a reduction in both step time and total time of a factor of 2 have been noted for a number of test cases.

2.3 Wake Cutting

Unusual but not negligable in conventional aircraft configurations, impingement of the wake from one part of the configuration on another is commonplace in helicopters and unavoidable in most modes of flight. Consequently, any analysis probing the time domain must not only be able to accommodate impingement of wakes on the surface but also be able to distort, or even tear the wake as it passed downstream.

Wake development, including impingement, which forced unnatural constraints such as rigid stream-wise prescribed wakes on early panel methods, was built in as one of the conditions that had to be accomodated in program VSAERO. Ref. 41 discusses the development of the technique and the way in which the doublet/source model in VSAERO (and, by extension, in the time-stepping program) handle wake impingement and the behavior of portions of the surface embedded in wakes.

In the unsteady program the wake development is determined by a simple integration of the local velocity field at the preceding time step, Figure 3. Two distinct types of wake/surface intersections emerge as a result of this procedure and they dictate different responses on the part of the program.

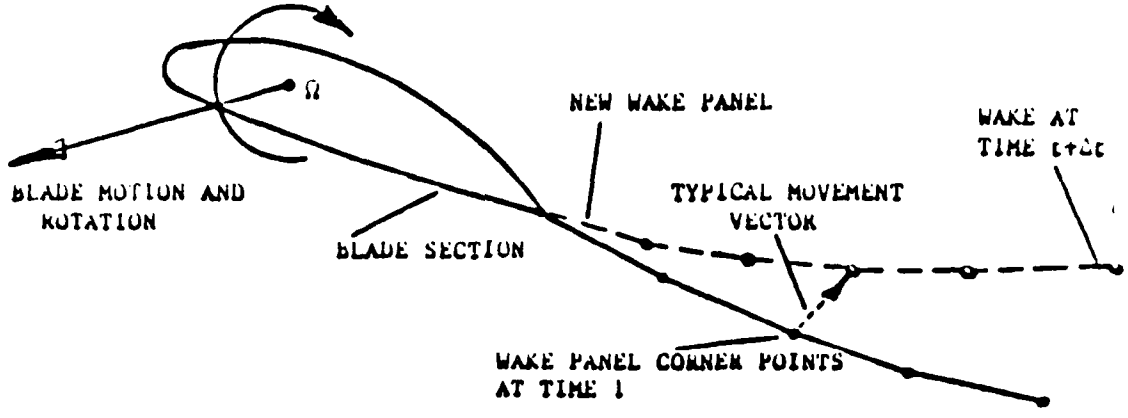

Fig. 3. Wake Development Model.

In the first type, the grazing encounter shown in the sketch below, the wake and blade have advanced a step from their previous position and the calculation procedure shows that a wake node, the joint between two wake panels, falls within the surface. This, of course, is unnatural and the program, Within guidelines involving the relative angle of the encounter, will simply move the node outside the surface in a direction along the local normal.

In the other extreme, the direct cutting encounter, the blade will physically penetrate the wake sheet as in the next sketch.

In this type of encounter the wake, after initially deforming along its leading edge, appears to tear (although flow visualization data of this type of encounter is rare, the laser survey results of Ref. 50 tend to support the assumption). Within the constraints of the model this kind of event can be handled in one of two ways, either one representing (with variation in refinement) what appears to happen in practise.

The simplest approach is merely to cancel out the strength of the panels impacted (penetrated) by the surface. This would leave, as in the next sketch, a raw edge in the sheet which would subsequently deflect under its own influence. The surface panels would pick up the jump in singularity strength associated with the raw edge and contribute (an image of the edge) to the local distortion.

The second more refined approach results from the way in which the wake panels are triangulated in the solution. In this case the edges of the cut region would pick up the appropriate diagonal of the wake panel as in the next sketch.

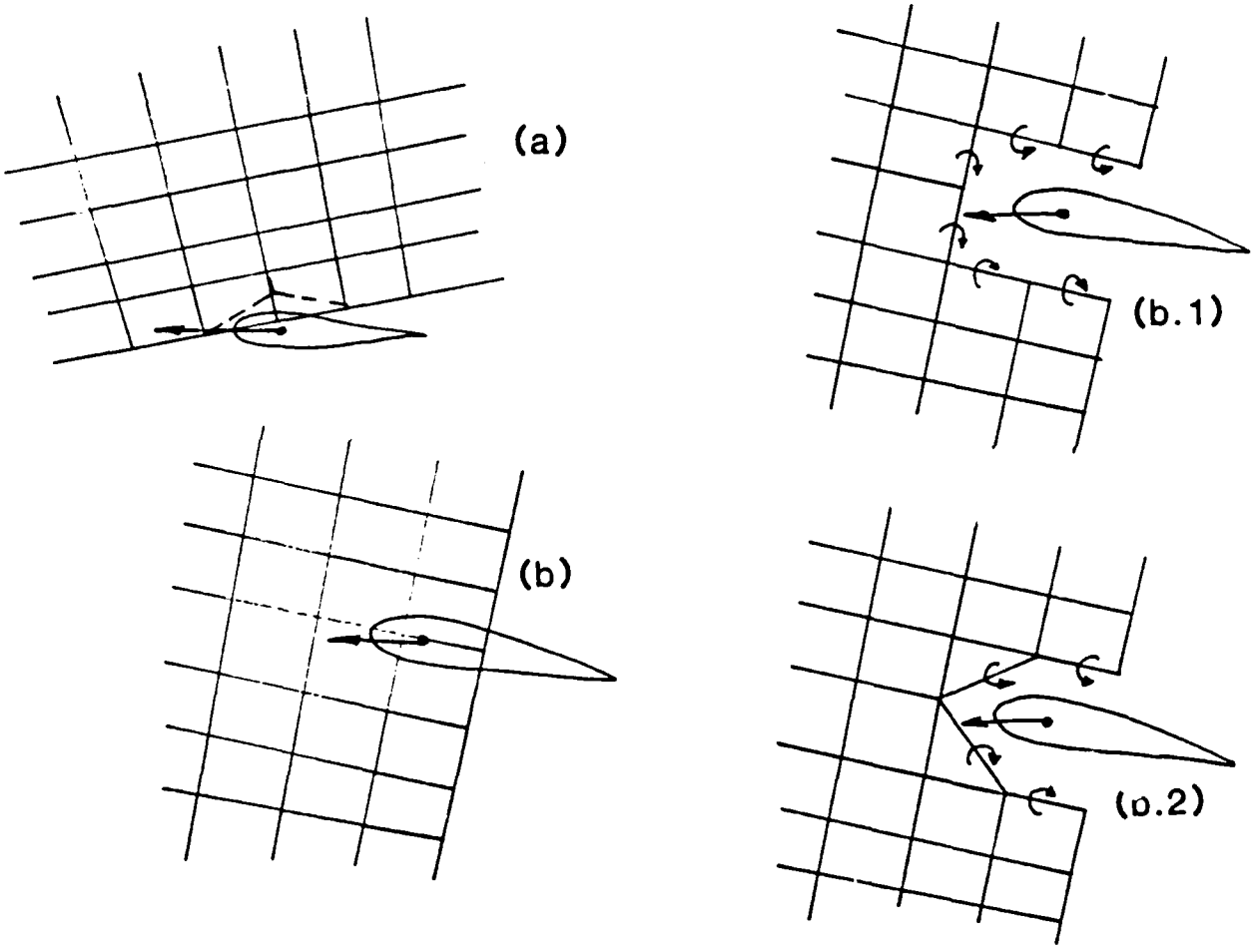
(a)
(b)
(b.1)
(b.2)

3.0 PROGRAM VALIDATION

Because of the large experimental data base available from model and full-scale wind tunnel and flight sources and the depth to which it has been explored in previous analytical studies, the H-34 rotor was chosen for the initial program validation. The rotor has four blades of 28 ft. radius. These blades are linearly twisted (-8 Degrees) and are of constant chord. The blades are fully articulated and, in practise, have cyclic and collective pitch change.

To complement the H-34 rotor a simplified version of the NASA Ames 40- x 80-foot wind tunnel rotor test module was selected for the initial study. This was chosen because, as well as being a representative helicopter shape, it was easily generated in the panel model and was free from configuration clutter which could confuse the early results from the analysis. The mounting struts, the strut fairing and the rotor head were also omitted from the analysis, although a rotor head mass was used in the isolated rotor calculation model. Figure 4 shows a view of the panel model with the rotor set at the position from which the calculation was started.

For these proof-of-concept runs, a balance was struck between providing panel density sufficient to resolve flow details and the long execution times involved if large panel numbers are used. For the body, essentially a body of revolution, a total of 276 panels were used. These were arranged in 12 columns of 23 panels, with the density being set to give 8 panels from the nose to the maximum girth and 12 from that point to the base. There were 3 panels inside the base. The circumference was divided into 12 panels. Each blade was paneled with a total of 8 panels chordwise, 4 lower, 4 upper, and 5 spanwise. Each tip and root was covered with a cap. This paneling, especially on the blades, may seem somewhat crude, but experience with earlier models has shown it to be adequate for carrying out proof-of-concept testing. For detailed loads work, of course, many more panels would be required. Typically 10 to 15 spanwise and 6 or 8 on lower and upper surfaces would be adequate. The panels would be spaced, as they are in the present model, such that they follow a cosine distribution towards tip and leading edge.

3.1 Isolated Rotor

Since any analysis developed to model body/rotor combinations must also be able to calculate the behavior of isolated rotors this was felt to be a required step. Working with a two-bladed H-34 rotor (with no applied cyclic pitch or blade flapping permitted), a study was made of sensitivity to time-step size. An advance ratio of 0.15 was chosen as typical. Time-step size was varied as the calculation progressed with 12 steps per revolution for the first two revolutions, 24 steps in the third revolution and 36 steps in the fourth revolution. The calculated wake shapes, tip vortex panel only is shown for clarity, are drawn in Figure 5. The first view, Figure 5(a), is an obligue view from the rear and shows that despite the crude paneling and large time steps of the first two revolutions, the wake exhibits all the characteristics that have become familiar from the flow visualization literature, Refs. 10 and 11 are typical. In this view and the overhead and side views that follow, Figures 5(b) and (c), the tendency of the edges of the wake to roll up into distinct bundles is clearly seen. Clear, too, is the depression of the center of the wake as the development progresses downstream. The wake convection angle is consistent with the calculated thrust level.

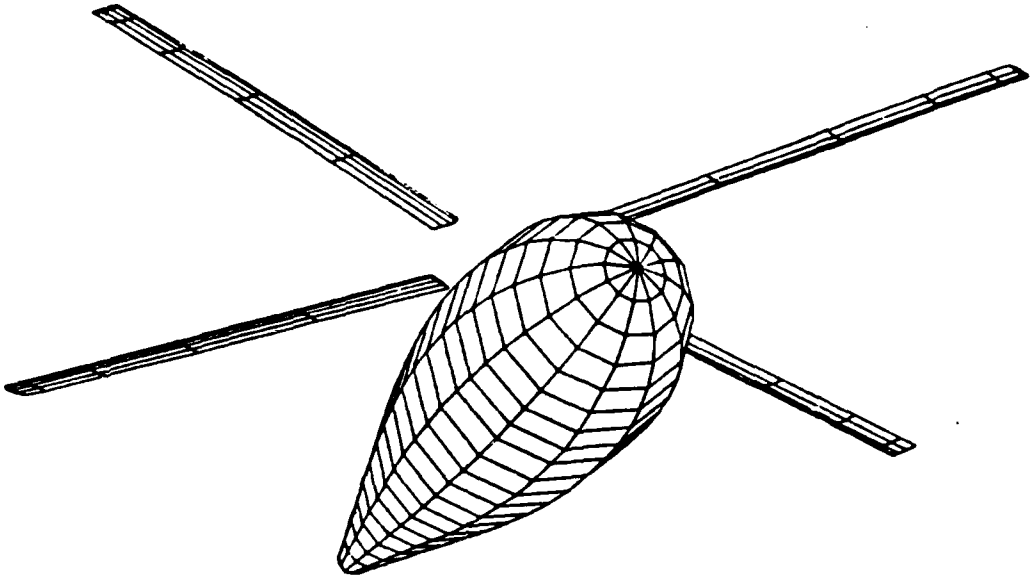

Fig. 4. Panel Model of H-34 Rotor and Wind Tunnel Module.

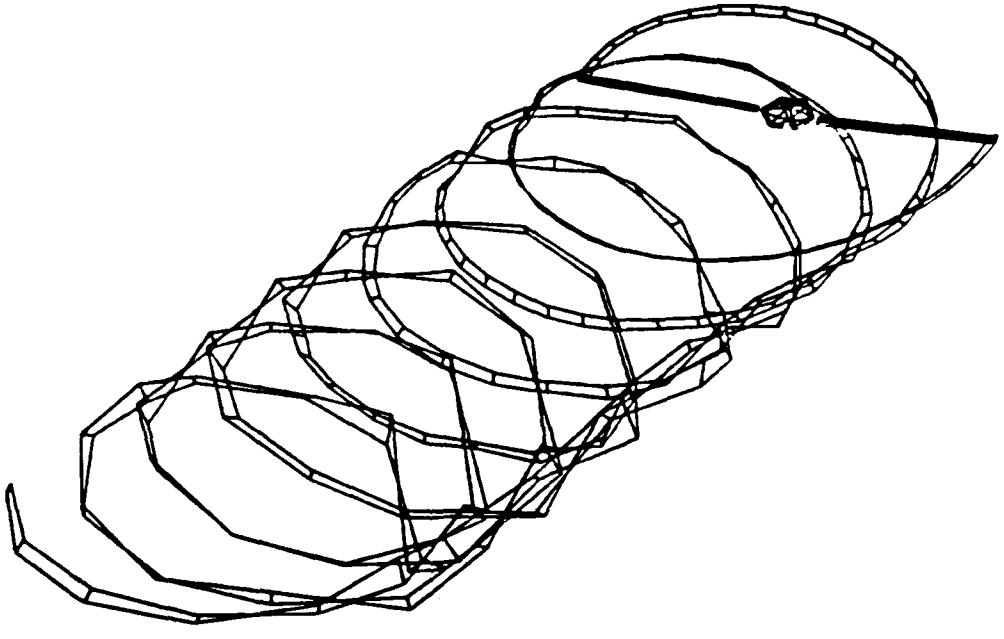

(a) Oblique View

Fig. 5. Calculated Relaxed Wake Two-Bladed H-34 Rotor Disc Loading 2.5 lb./ft.^{2}, 0.15 Advance Ratio.

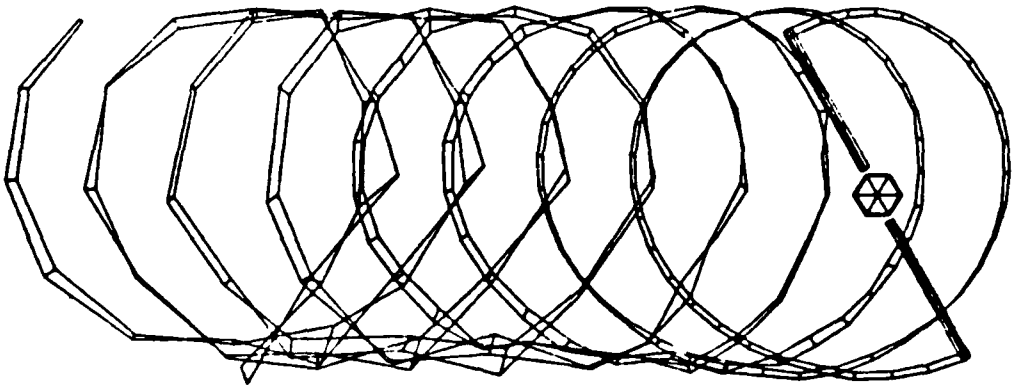

(b) Overhead View

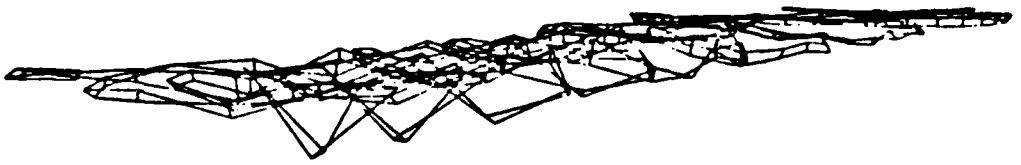

(c) Side View

Fig. 5. Concluded.

The next sequence of pictures, Figures 6(a) through (d) from time steps 65 through 68, shows a series of overhead view highlighting the interference between the advancing blade and the preceding blade tip vortex, in reality as shown here, the rolling up leading edge of the sheet laid down by the preceding blade. In this sequence, the sheet edge passes under the third blade section with center at about 2/3 radius. Figure 7 shows the history of the lift on that section for all four cycles with the vortex passage incident pointed to in Figure 6 highlighted. The progression of the vortex inboard, along the blade, is very clearly seen. Figure 8 shows the local surface pressure on the panels above and below the leading edge over the same time peaiod and again the vortex passage shows clearly as a radical change in pressure levels. It is also interesting to note from the last plot, that even the crude twelve-step revolution produces evidence of the blade passing vortex encounter. This is an example of a pass where the blade and vortex are at a large relative angle.

Figures 6(c) and (d), at time steps 67 and 68, show that the retreating blade is undergoing a parallel passing incident. Here the evidence is subtler, but is still unmistakable in the upper surface pressures beginning at steps 48 (time 0.7 secs.) and again at step 82/83, (time 0.96 secs.) in Figure 8. This is when the blade from which the pressure data is taken passes through the position of the retreating blade in Figure 6(e). The blade chordwise pressure distribution at steps 67 and 68,before and after passage, are shown in Figure 9. Despite the crude model (4 panels chordwise), representative distributions are seen. Attention should be drawn to Figure 10 which shows the overall thrust coefficient of one blade for the four cycles. The starting process is very quickly established as evidenced by the only small changes as the four cycles presented develop. The only substantial variation is the extra detail introduced by increasing the steps per cycle from 12 in the first two cycles to 24 in the third, and finally to 36. The calculation starts with the primary blade (the one for the histories) at $\Psi = 300°$.

To complete the data for the isolated rotor case, Figure 11 presents the full calculated wake at the end of time-step 85 as viewed from above. The convoluted trajectory of the inboard wake filaments are evident.

3.2 Body/Rotor

Because of problems associated with the excessive motion of the wake relative to the body when large time steps (12/revolution) were used, it was not possible to start the body/rotor cases with the 12/revolution steps used in the isolated rotor cases. In this case, 24/revolution steps were found to be a maximum acceptable size. The case presented was allowed to develop up to time step 49, or 2 24-step revolutions, show detail adequate to validate the method's performance.

Figure 12(a) through (c) shows, as in the earlier series, the body/rotor combination this time after 48 time steps. Again, only the tip-edge panel for the wake has been drawn. The wake calculated including the effect of the body has, as would be expected, all the features associated with the isolated wake. However, some significant differences exist. The wake shows the same tendency to bundle along the edges and, from the side view, the same looping behavior is present, but the influence of the body upwash is very obvious in the way in which the wake in the third quadrant is carried aft much higher than for the rotor alone. The wake appears, in fact, to pass over the retreating blade close to the body.

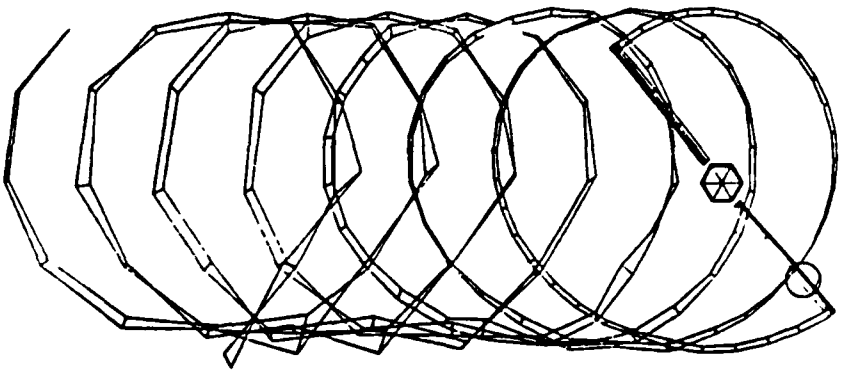

(d) Step 68

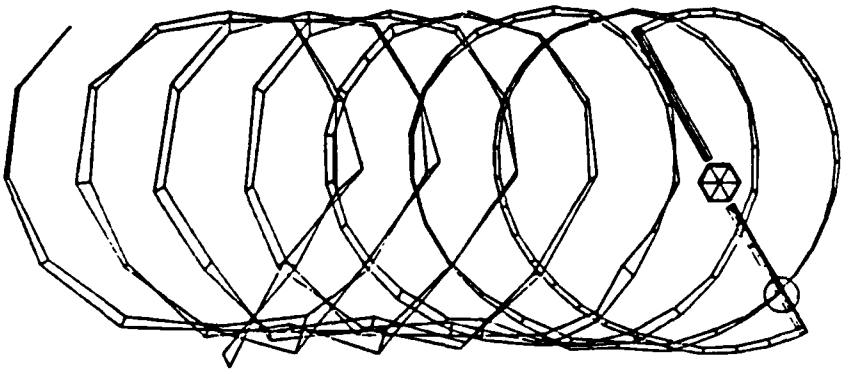

(c) Step 67

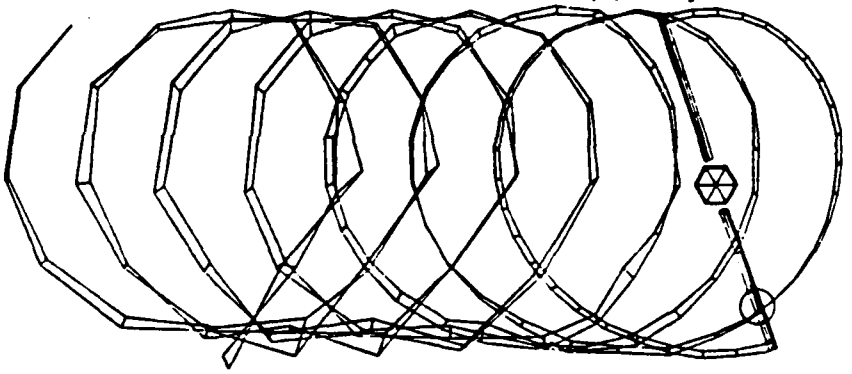

(b) Step 66

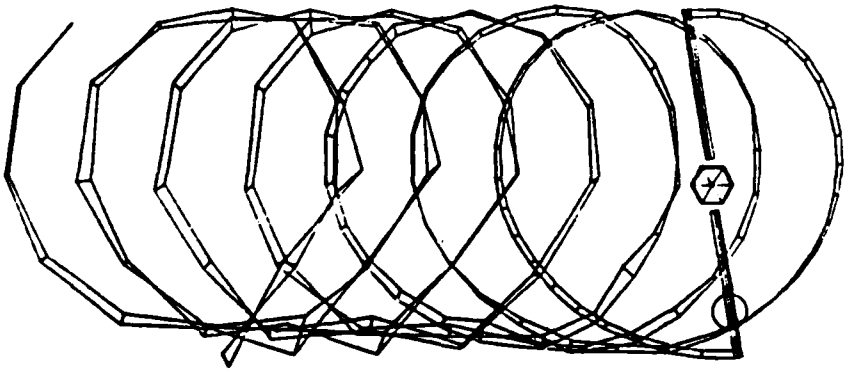

(a) Step 65

Fig. 6. Overhead View of Two-Bladed Rotor; Time Steps 65-68.

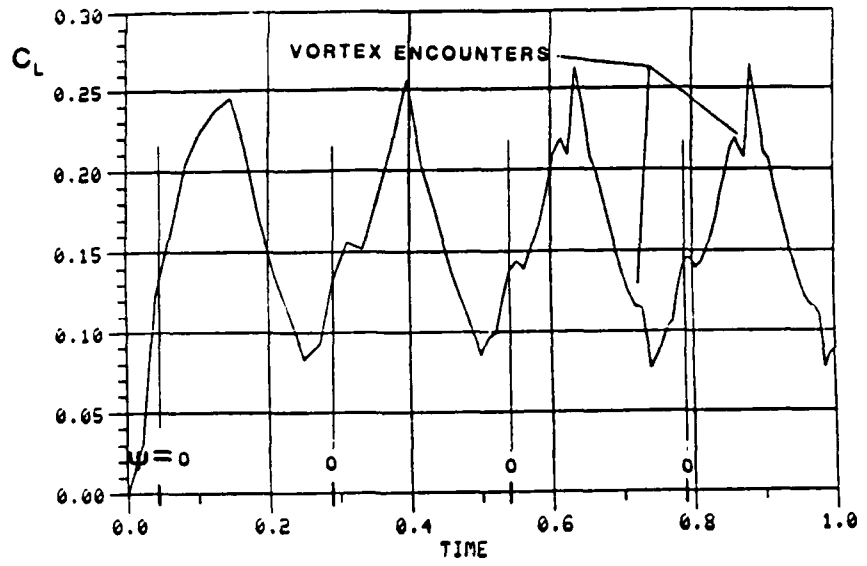

Fig. 7. Time History of Section C_L Mid-Span on Two-Bladed H-34 Rotor; μ= 0.15, DL = 2.5 lb./ft.^{2}. Four Blade Revolutions.

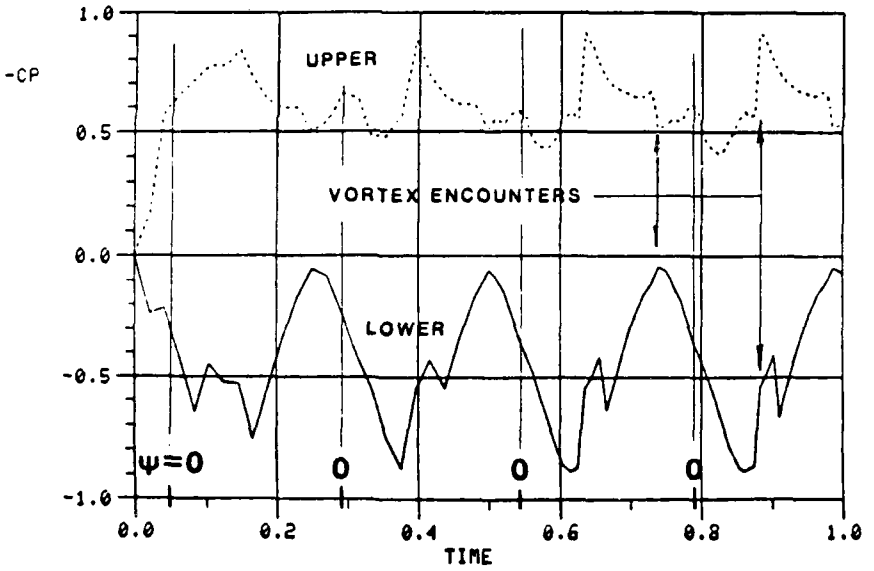

Fig. 8. Time History of Blade Section Leading-Edge Pressures at Mid-Span; H-34 Rotor: Two Blades, 0.15 Advance RAtio

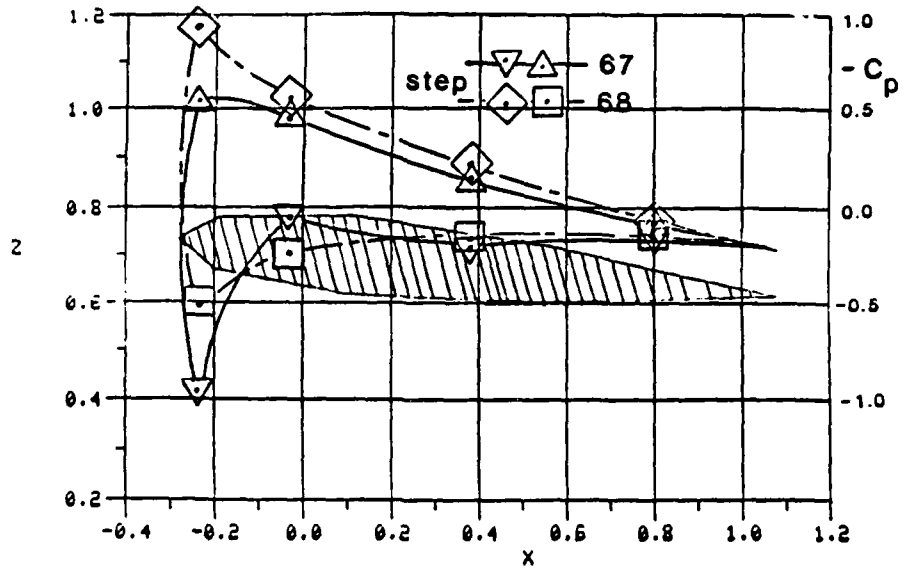

Fig. 9. Blade Section Cp at Mid-Span for Time Steps 67 and 68; Two-Bladed H-34 Rotor, μ = 0.15.

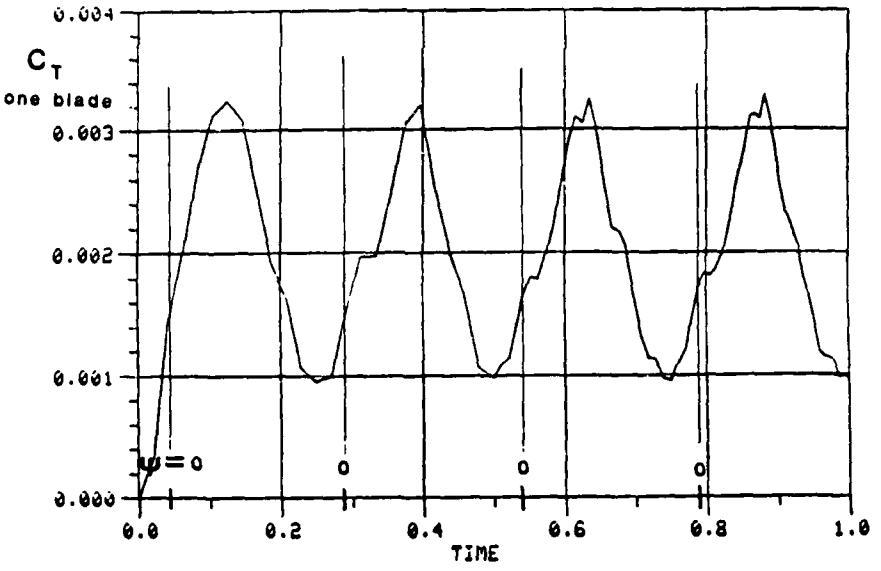

Fig. 10. Time History of Total Thrust Coefficient; H-34 Rotor, Two Blades, μ = 0.15, DL = 2.5 lb./ft.^{2}.

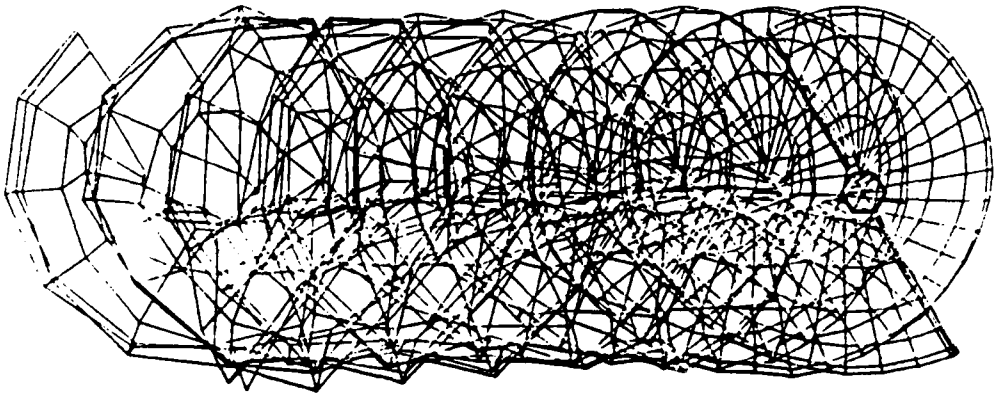

Fig. 11. View of Full Wake--H-34 Two-Bladed Rotor; 0.15 Advance Ratio.

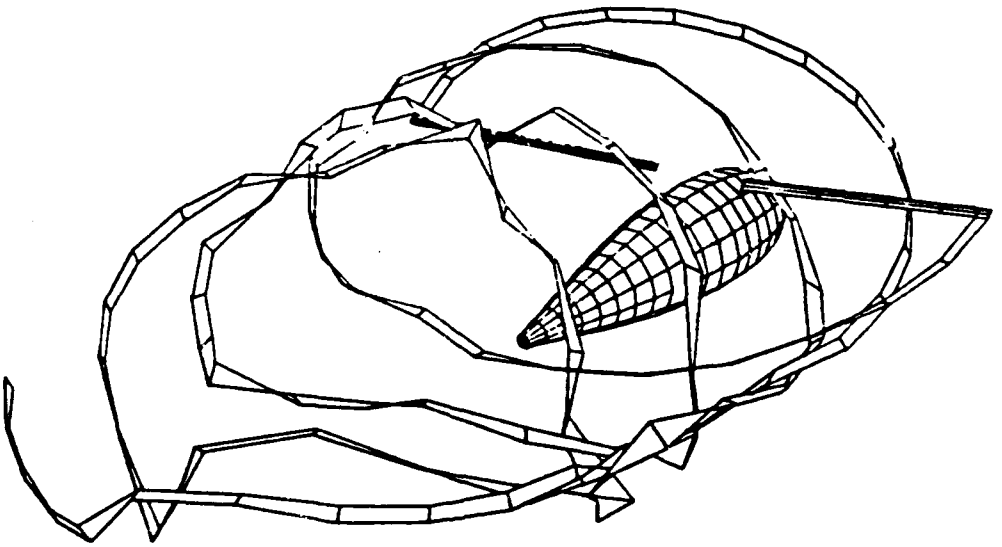

(a) Oblique View

Fig. 12. H-34 Two-Bladed Rotor with Test Module; 0.15 Advance Ratio, DL = 2.5 lb./ft.^{2}. Tip Vortex Only Shown for Clarity.

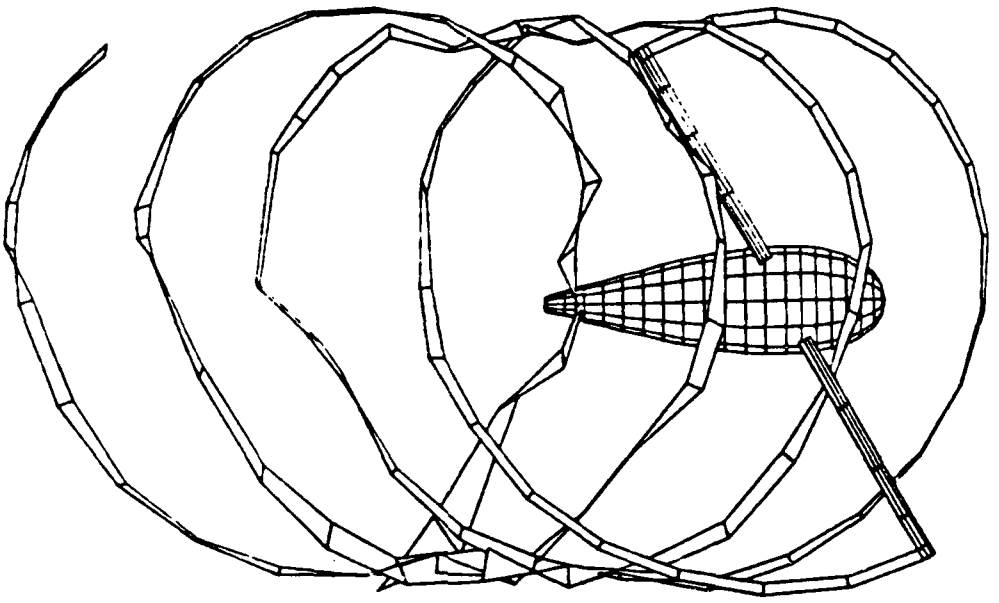

(a) Overhead View

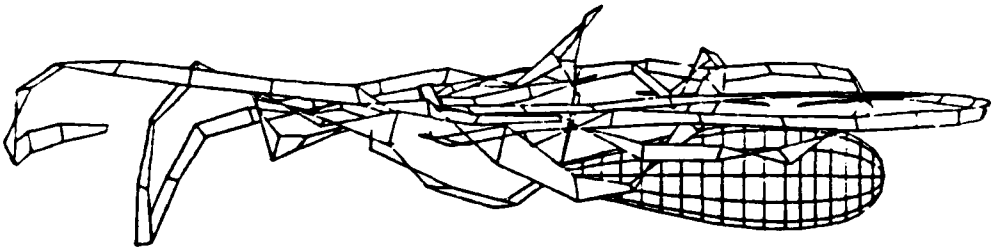

(b) Side View

Fig. 12. Concluded.

With this in mind, it is not surprising that the cyclical variation of loading on the middle blade segment, Figure 13, and the corresponding blade leading-edge pressures, Figure 14, show a higher harmonic content while exhibiting the same general form as the earlier isolated rotor result. Figures 15(a) - (e) show the relative blade wake positions for time steps 33 through 41 and allow the correlation of the loads variation with blade/vortex relative position. As with the isolated rotor, there is a parallel encounter on the retreating side at about step 25 and again beginning at step 49. This time it is stronger because of the relatively higher position of the wake. It should be noted that at only 24 steps per revolution some of the resolution is lost. Note how the vortex encounters between steps 33 and 35 blend into one event.

The body loads also show a strong harmonic content associated with blade passage and with tip vortex convection. Of the two, at least for this combination of blade fuselage spacing and loading, the vortex effect is stronger. Figure 16 tracks the surface pressure at three locations on the body as a function of time step. The three locations are: (a) roughly half way from the nose to the maximum thickness; (b) just ahead of the maximum thickness: and (c) just aft of the maximum thickness.

The rotor begins at time step one with the primary blade at -60 degrees (in the fourth quadrant) and the secondary blade at +120 degrees azimuth and the passage of both blades over the fuselage is clearly seen as perturbation in the local Cp values at steps 5 and 17. The next passages at step 29 and then at 41 are overshadowed by the passage of the tip vortex laid down around the front of the disc. The first of these arrives at A at time step 24 although it is felt well ahead of its arrival. The first leading-edge disturbance arrives at B at about time step 28 and at C about step 36. It should be noted here that the Cp values in Figures 8, 14 and 16 are referenced to the rotor tip speed and should be multipled by $1/(0.15)^2$ to be returned to the aircraft flight speed reference. Figure 17 presents the time history of the surface velocity and shows the strong influence of the unsteady elements of the flow (the time rate of change of the surface doublet term) on the calculated Cp values. Note the high levels of lateral velocity and recall that $V_\infty = 0.15V_{ref}$. The reference velocity used is the rotor tip speed.

Given the levels of dynamic loading seen above at the local level, it is not surprising that the overall lift on the body fluctuates. Although small, the overall load variation is an appreciable fraction of the rotor average thrust coefficient (as much as 10%). It will be interesting to repeat the calculation at higher advance ratios.

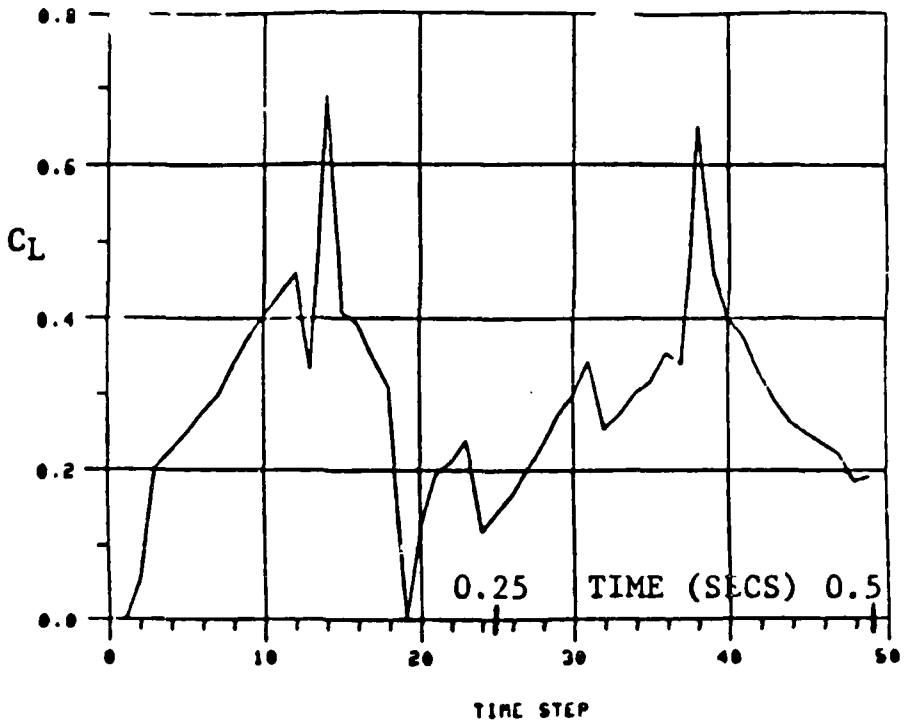

Fig. 13. Time History of Blade Section Lift Coefficient Mid-Span. H-34 Rotor, Two Blades with Test Module; 0.15 Advance Ratio.

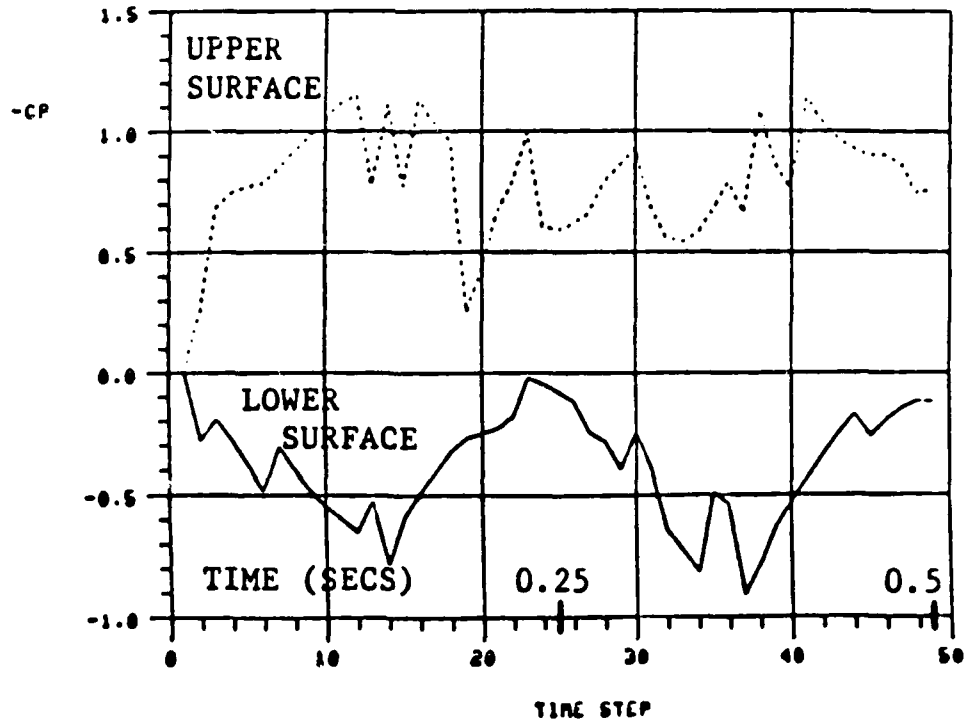

Fig. 14. Time History of Blade Section Leading-Edge Pressures at Mid-Span. H-34 Rotor, Two Blades with Test Module; 0.15 Advance Ratio

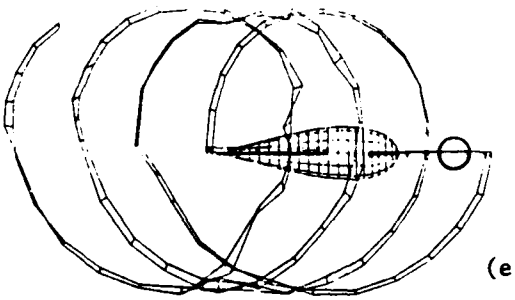

(e) Step 41

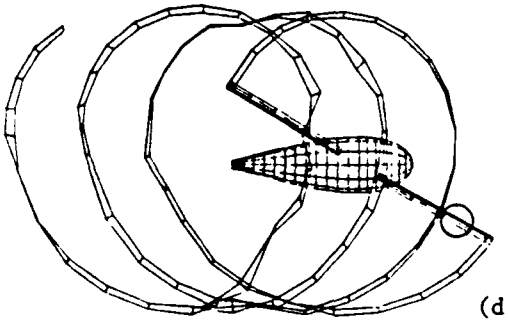

(d) Step 39

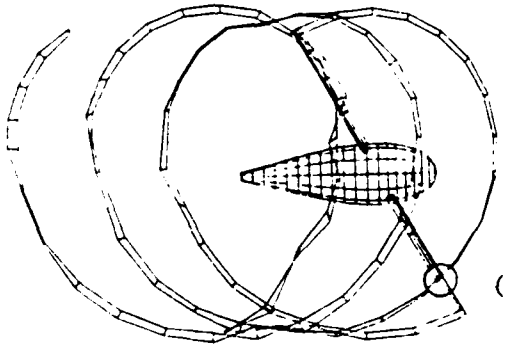

(c) Step 37

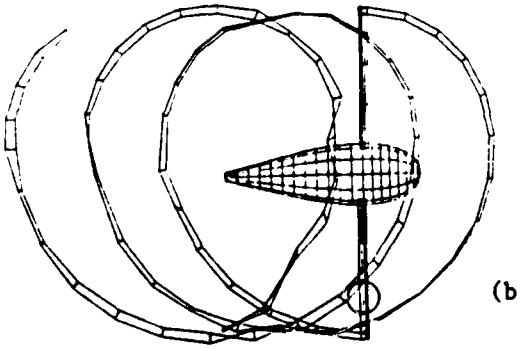

(b) Step 35

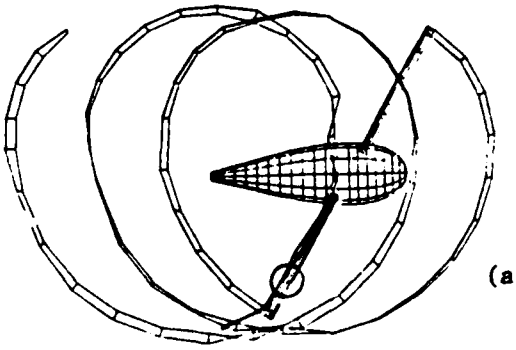

(a) Step 33

Fig. 15. Two-Bladed Rotor with Test Module. 0.15 Advance Ratio.

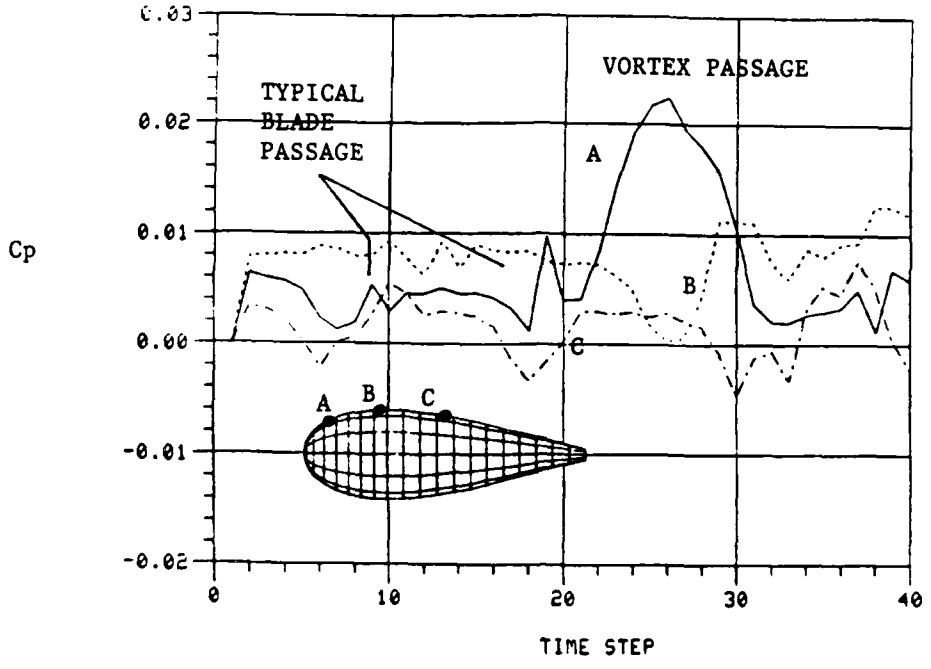

Fig. 16. Time History of Body Surface Pressures. H-34 Rotor, Two Blades with Test Module; 0.15 Advance Ratio.

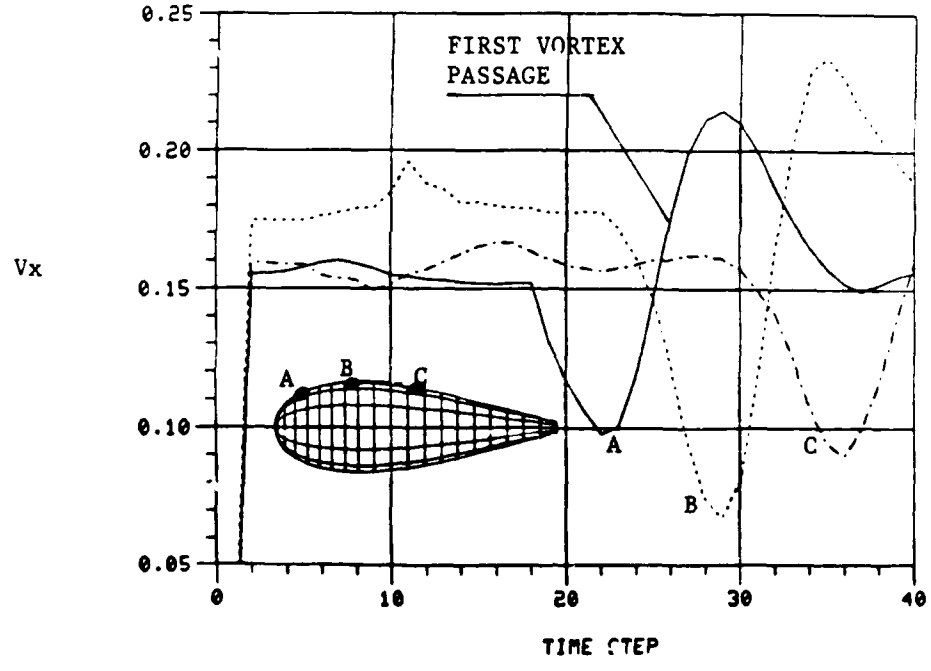

Fig. 17. Time History of Body Local Axial Surface Velocity; H-34 Rotor--Two Blades with Test Module, 0.15 Advance Ratio.

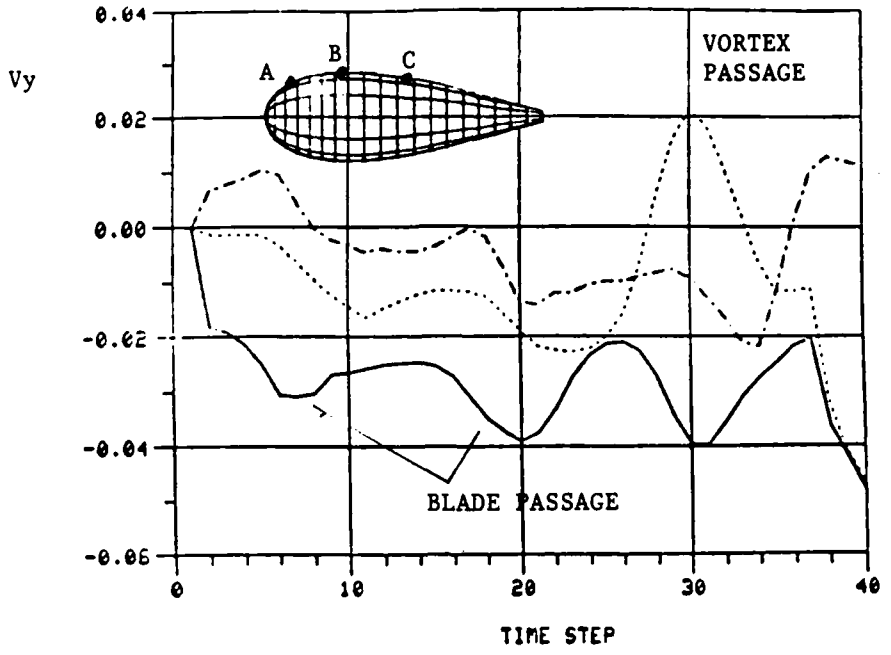

Fig. 18. Time History of Body Local Lateral Surface Velocity; H-34 Rotor-- Two Blades with Test Module, 0.15 Advance Ratio.

3.3 Propeller/Nacelle

Although wake/surface intersections are a strong possibility in this helicopter configuration discussed above they are inevitable in propeller installation problems and especially in nacelles where there is some protruding inlet structure. To examine the ability of the wake cutting scheme outlined in section 2 to handle this type of flow the model shown in figure 19 was developed.

This shows a co-axial installation with a typical four bladed propeller. The geometry was chosen not so much to model an existing propeller as it was to exercise the analytic model. Wakes are attached along the full blade trailing edge and as the propeller advances the wake streams out behind. Consequently wake/surface intersection is inevitable as the trailing sheet drifts aft with the inboard end being ingested by the inlet and the outer portions passing downstream in the clear.

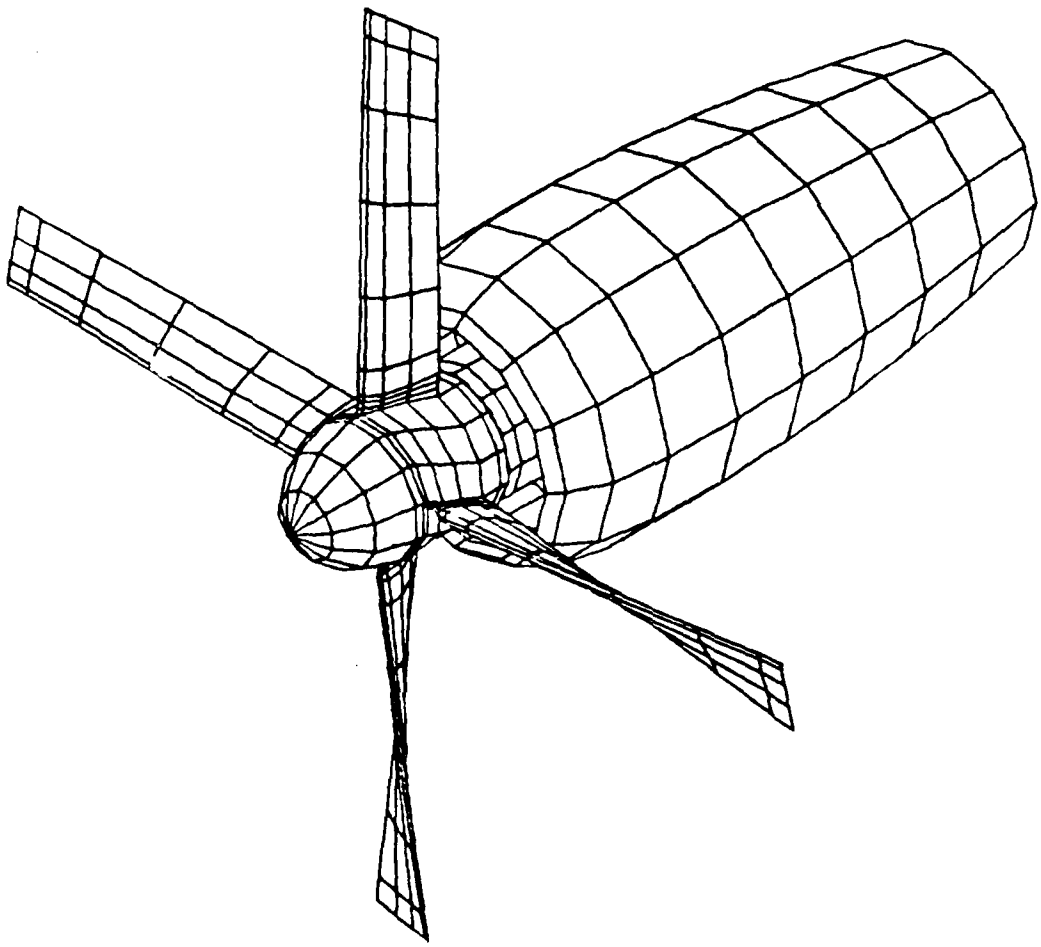

Fig. 19. Nacelle Panel Model with 4 Bladed Propeller.

Figure 20 illustrates this with one quarter of a turn of wake from one blade drawn in. The wakes from the other blades have been omitted for clarity. Figure 21 shows a closeup of the inboard portions of this wake with the "raw" edge around the deactivated panels darkened to emphasise the region. Panels once deactivated remain inactive as that region is converted down stream. It should be noted that this deactivation procedure is automatic and requires no input from this user. This applies also to the "nudge" procedure dealing with the glaring interference.

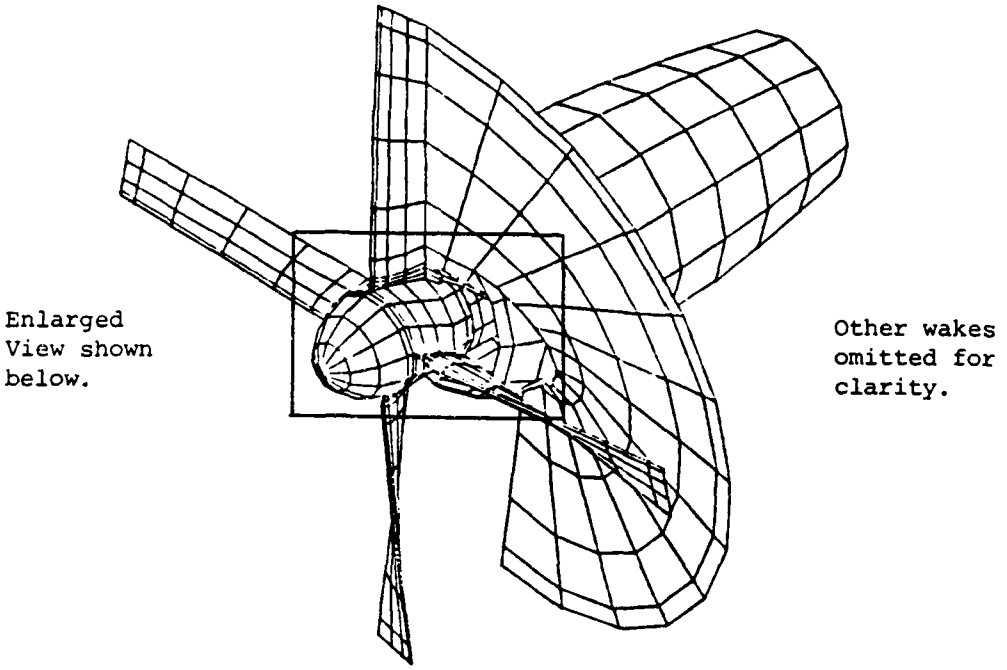

Fig. 20. Propeller Wake with Deactivated Panels in Root Region.

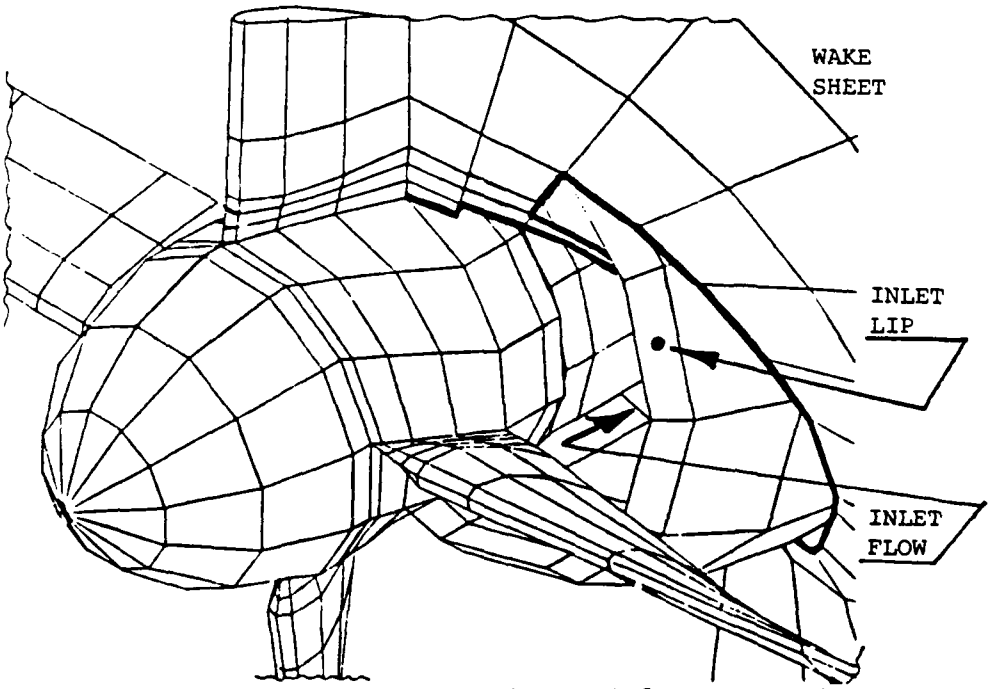

Fig. 21. Enlarged View of Detail from Figure 20.

It became evident at a very early stage in this study that substantial volumes of output would be generated. As an example, the roughly 400-panel, 48 time step analysis reviewed above generated a plot file for post processing of over 3 Mbytes. Evaluating an output file of that volume with conventional methods poses an intimidating problem. Thankfully, post-processing interactive color graphics routines, developed at AMI to support panel method applications, are available.

Extensive use was made of these routines, in particular, the color contour options, to explore quickly the details of the surface flow as it developed in time.

4.0 Conclusions and Plans for Future Work

An analysis has been developed which allows exploration of the details of the unsteady flow associated with generalized helicopter flight. Based on a well documented and widely accepted second generation low-order panel method the program carries out the solution into the time domain using a stepping procedure. At each step the program solves for the body and blade aerodynamics, including all the unsteady surface and wake motions, before moving on to the next step modifying the wake shape in the process. The program has been used to examine the temporal and spatial variation of both blade and fuselage airloads and has demonstrated that it not only can calculate dynamic loads but that it has an ability to capture flow details such as blade vortex interactions.

Plans for future development include exploration of ways to capture supercritical flow phenomena by local use of a field singularity rather than a surface singularity (this has already been demonstrated in a two-dimensional pilot code); the use of an unsteady viscous flow analysis (already operational in the fixed-wing version of the program) to calculate boundary layer and flow separation effects; inclusion of the full spectrum of blade motions, including elastic deflections and incorporation of rotor trim algorithms. The ultimate goal is the development of a model which can be "flown" through dynamic maneuvers, including flares and pull-ups, etc. outputting a complete description of both blade and body forces to whatever level of detail is desired. At the other end of the scale it is hoped that the analysis, operated with fine time steps and with locally denser paneling, will be able to produce radial and chordwise variations of local loading in enough detail to be of benefit to aid in improvements in noise prediction.

5.0 References

1. Glauert, H., "A General Theory of the Autogyro", ARC R&M 1111, November 1926.

2. Glauert, H. and Lock, C.N.H., "A Summary of the Experimental and Theoretical Investigations of the Characteristics of an Autogiro", ARC R&M 1162, April 1928

3. Wheatley, J.B., "An Aerodynamic Analysis of the Autogiro Rotor with a Comparison between Calculated and Experimental Results", NACA Report 487, 1934

4. Harris, F.D., "Rotary Wing Aerodynamics. Historical Perspective and Improtant Issues", Presented at the American Helicopter Society (Southwest Region) National Specialists' Meeting on Aerodynamics and Aeroacoustics, February 1987.

5. Piziali, R. and DuWaldt, F., "A Method for Computing Rotary Wing Airload Distribution in Forward Flight", Cornell Aero. Lab., Report BB-1495-S-1, TCREC TR 62-44, November 1962

6. Sadler, S.G., "Development and Application of a Method for Predicting Rotor Blade Air Loads", Rochester Applied Science Associates, NASA CR-1911, December 1971

7. Crimi, P., "Theoretical Prediction of the Flow in the Wake of a Helicopter Rotor", Cornell Aero. Lab. Report No. BB-1994-S-1, September 1965

8. Miller, R., "on the Computation of Airloads Acting on Rotor Blades in Forward Flight", J.A.H.S., Vol. 7. No. 2, April 1962

9. Scully, M.P., "A Method of Computing Helicopter Vortex Wake Distortion", M.I.T. Aeroelastic and Structures Research Lab. TR 138-1, June 1967

10. Landgrebe, A.J. and Bellinger, E.D., "An Investigation of the Quantitative Applicability of Model Helicopter Rotor Wake Patterns Obtained from a Water Tunnel", USAAMRDL TR-71-69, December 1971

11. Landgrebe, A.J. and Egolf, T.A., "Prediction of Helicopter Induced Flow Velocities Using the Rotorcraft Wake Analysis", AHS Forum, 1976.

12. Clark, D.R. and Leiper, A.C., "The Free Wake Analysis, Amethod for the Prediction of Helicopter Rotor Hovering Performance", J.A.H.S, Vol. 15, No. 1, January 1970.

13. Bliss, D.B., Wachspress, D.A. and Quackenbush, R.T., "A New Approach to the Free Wake Problem for Hovering Rotors", Proc. 41st Annual Forum of the American Helicopter Society, Ft. Worth, Texas, May 1985.

14. Quackenbush, T.R., "Computational Studies in Low Speed Rotor Aerodynamics and Aeroacoustics, Arlington, Texas, February 1987.

15. Gormont, R.E., "A Mathematical Model of Unsteady Aerodynamics and Radial Flow for Application to Helicopter Rotors", USAAMRDL TR 72-67, May 1973

References Cont.

16. St. Hilaire, A.O., Carta, F.O., and Jepson, W.D., "The Influence of Sweep on the Aerodynamic Loading of an Oscillating NACA 0012 Airfoil", Presented at the 35th Annual National Forum of the American Helicopter Society, Washington, D.C., May 1979

17. Hess, J.L. and Smith, A.M.O., "Calculation of Non-Lifting Potential Flow about Arbitrary Three-Dimensional Bodies", Douglas Aircraft Co., Inc., Report No. E.S. 40622, March 1962

18. Rubbert, P.E. and Saaris, G.R., "Review and Evaluation of a Three-Dimensional Lifting Potential Flow Analysis Method for Arbitrary Configurations", AIAA Paper No. 72-188, January 1972.

19. Woodward, F., Dvorak, F. and Geller, E., "A Computer Program for Three-Dimensional Lifting Bodies in Subsonic Inviscid Flow", USAAMRDL TR-74-18, April 1974.

20. Ashley, H., Widnall, S.E. and Landahl, M.T., "New Directions in Lifting Surface Theory", AIAA J., Vol. 3, No. 1, 1965

21. Ashley, H. and Rodden, W.P., "Wing-Body Aerodynamic Interaction", Annual Review of fluid mechanics, Vol. 4, 1972.

22. Dojodihardjo, R.H. and Widnall, S.E., "A Numerical Method for the Calculation of Nonlinear, Unsteady Lifting Potential Flow Problems", AIAA J, Vol. 7. No. 10, October 1969.

23. Summa, J.M., "Unsteady Potential Flow about Wings and Rotors Started Impulsively from Rest", Unsteady Aerodynamics, Kinney, R.B., ed., (Proc. Symposium at University of Arizona) March 1975

24. Johnson, W., Helicopter Theory, Princeton University Press, Princeton, N.J., 1980

25. Dat, R., "Development of the Basic Methods Nedded to Predict Helicopter Aeroelastic Behavior", Presented at Eight European Rotorcraft Forum, Aix-en-Provence, France, 1982

26. Dat, R. and Tran, C.T., "The Use of Advanced Aerodynamic Models in the Aeroelastic Computations of Helicopter Rotors", Paper No. 56, Presented at 12th European Rotorcraft Forum, Garmisch-Partenkirchen, West Germany, 1986

27. Arieli, R. and Tauber, M.E., "Computation of Subsonic and Transonic Flow about Lifting Rotor Blades", AIAA Paper 79-1667, August 1979

28. Tauber, M.E., Hicks, R.M., "Computerized Three-Dimensional Aerodynamic Design of a Lifting Rotor Blade", Proc. 36th Annual Forum of the American Helicopter Society, May 1980

29. Jameson, A., "Iterative Solution of Transonic Flows over Airfoils and Wings Including Flows at Mach 1", Communications on Pure and Applied Mathematics, 27, 197

30. Caradonna, F.X. and Philippe, J.J., "The Flow over a Helicopter Blade Tip in the Transonic Regime", Vertica, 2, 1978

References Cont.

31. Caradonna, F.X., Tung, C., and Desopper, A., "Finite Difference Modeling of Rotor Flows Including Wake Effects", J.A.H.S., April 1984

32. Caradonna, F.X., Tung, C., "Experimental and Analytical Studies of a Model Helicopter Rotor in Hover", NASA TM 81232 (or USAAVRADCOM TR-81-A-23), September 1981.

33. Egolf, T.A. and Sparks, S.P., "A Full Potential Rotor Analysis with Wake Influence Using an Inner-Outer Domain Technique", Proceedings 42nd Annual Forum of the American Helicopter Society, June 1986.

34. Sankar, L.N. and Tung. C., "Euler Calculations for Rotor Configurations in Unsteady Forward Flight", Presented at 42nd Annual Forum of the American Helicopter Society, Wahington, D.C., June 1986

35. Wake, B.E. and Lakshmi, N.S., "Solutions of the Navier-Stokes Equations for the Flow About a Rotor Blade". Presented at the American Helicopter Society Specialists' Meeting on Aerodynamics and Aeroacoustics, Arlington Texas, 1987.

36. Sheridan, P.F., "Interactional Aerodynamics of the Single Rotor Helicopter Configuration", USARTL TR 78-23, September 1978

37. Landgreve, A.J., Moffitt, R.C. and Clark, Dr.R., "Aerodynamic Technology for Advanced Rotorcraft", J.A.H.S., Vol. 22, No. 2, April 1977 and No. 3, July 1977.

38. Sheehy, T.W., "A Simplified Approach to generalized Helicopter Configuration Modeling and the Prediction of Fuselage Surface Pressures", J.A.H.S., Vol. 21, No. 1, January 1976

39. Huber, H. and Polz, G., "Studies of Blade to Blade and Rotor-Fuselage-Tail Interferences", AGARD Conference Reprint, May 1982

40. Stricker, R. and Polz, G., "Calculation of the Viscous Flow around Helicopter Bodies", Paper Presented at the Third European Rotorcraft and Powered Lift Forum, Aix-en-Provence, France, September 1977.

41. Clark, D.R., "Study for Prediction of Rotor-Wake/Fuselage Interference: Parts I and II" NASA CR-16653-I and NASA CR-16653-II, November 1983

42. Clark, D.R., "Analysis of the Wing/Rotor and Rotor/Rotor Interactions Present in Tilt-Rotor Aircraft", Paper Presented at International Conference on Rotorcraft Basic Research, ARO, Durham, N.C. February 1985

43. Cantaloube, B., "Numerical Calculation of Rotor Performance in Real Flight configurations", Paper Presented to the International Conference on Basic Research, ARO, Durham, N.C., February 1985.

44. Maskew, B., "Prediction of Subsonic Aerodynamic Characteristics: A Case for Low-Order Panel Methods", J. Aircraft, Vol. 19, No. 2, February 1982.

45. Maskew, B., "Influence of rotor Blade Tip Shape on Tip Vortex Shedding--An Unsteady Inviscid Analysis", Paper 80-6 in Proc. 36th Annual AHS Forum, May 1980.

References Cont.

46. Katz, J. and Maskew, B., "Unsteady Aerodynamic Model for Complete Aircraft Configurations", Paper Presented at AIAA Atmospheric Flight Mechanics Conference, Williamsburg, Virginia, August 1986

47. Maskew, B. and Dvorak, F.A., "Prediction of Dynamic Separation Characteristics of General Configuarions", AIAA-86-1813, June 1986

48. McCroskey, W.J., Spalart, P.H., Laub, G.H., Maisel, M.D. and Maskew, B., "Airloads on Bluff Bodies with Application to the Rotor-Induced Downloads on Tilt-Rotor Aircraft", Vertica, Vol. 9, No. 1, 1985

49. Clark, D.R. and Maskew, B., "Use of Computer Models in Helicopter Drag Prediction", Presented at the AH S Specialists' Meeting on Aerodynamics and Aeroacoustics, Arlington, Texas, February 1987

50. Brand, A., Komerath, N.M. and McMahon, H.M., "A Laser Sheet Technique for Visualizing an Incompressible Vortex Wake", Paper AIAA-88-0192, January 1988

6.0 PERSONNEL

Technical work was carried out exclusively by David R. Clark and Dr. Brian Maskew, both full time employees of Analytical Methods Inc. No part of this work was used toward any advanced degree.

7.0 ASSOCIATED PUBLICATIONS

Preliminary results from this work were presented as part of the 2nd International Rotorcraft Basic Research Conference held at the University of Maryland, February, 1988. This meeting was sponsored in part by the Army Research Office.